

Research Article

Hasan A. Ajel*, Haider S. Al-Jubair and Jaafar K. Ali

An experimental study on vibration isolation by open and in-filled trenches

<https://doi.org/10.1515/eng-2022-0011>

received September 09, 2021; accepted December 31, 2021

Abstract: The mitigation of vibrations due to a harmonic load induced by a mechanical oscillator is studied experimentally. The vertical components of soil particle velocities are measured (via geophones) at different locations apart from the source, where various frequencies (30–70 Hz) are generated. For normal conditions where no mitigation means are used, it is found that the measured peak particle velocities are proportional to the excitation frequencies. The mitigation effect of constructing an active (near source) open (0.4 m wide × 3 m long × 2 m deep) trench barrier is also studied. The measurements revealed velocity increase at the points in front of the trench due to the reflected waves. This increase is proportional to the vibration frequency. Although the presence of the barrier greatly reduced the peak particle velocities beyond it, it is found that the efficiency of screening is more pronounced at high vibration frequencies. Increased and fluctuated trends of the amplitude reduction ratio are reported away from the barrier. It is realized that passive (near target) screening is less effective for all frequencies except at 30 Hz. Active and passive trenches, filled with native soil–rubber mixture at various ratios (20–40% rubber), are also considered. The rubber material is in a form of tire chips purchased from the Unit of Recycling Scrap Tires in Al-Diwaniyah Tires Factory. Although the in-filled trenches are less effective in screening the vibrations, similar trends and behavior to the open trenches are noted. It is found that the mitigation efficacy is increased with the rubber content.

Keywords: vibration screening, vibration mitigation, in-filled trenches, rubber material, scrap tire

1 Introduction

Controlling the vibrating energy coming into a sensitive zone is called vibration screening [1]. Efficient vibration screening can be achieved through proper surface wave interception, scattering, and diffraction by using barriers such as open trenches, filled concrete or bentonite trenches, sheet pile walls, and rows of solid or hollow concrete or steel piles. Active isolation (at source) and passive isolation (distance screening) schemes may be used in the mitigation of elastic waves by trenches. Different parameters are used to describe the amount of screening regarding vibration components (displacement, velocity, or acceleration). The effectiveness of screening can be measured with and without the wave barrier, depending on the ground motion observed. Amplitude reduction factor (A_r) is computed by normalizing the post-trench installing amplitude of vertical ground motion at selected points ($(A_r)_{\text{After}}$), by the amplitude of vertical ground motion at the same points before trench placing ($(A_r)_{\text{Before}}$), calculated on the ground surface [2]. The ratio of amplitude reduction is then given by

$$A_r = \frac{(A_r)_{\text{After}}}{(A_r)_{\text{Before}}} \quad (1)$$

Many research articles were published regarding the experimental investigation of the vibration mitigation capabilities of trench wave barriers [3–8].

The main objective of this work is to study the effectiveness of in-filled trenches as wave barriers utilizing locally available (cheap) filling materials. The approach is presented as follows:

- A-Establishing the wave propagation characteristics of Basrah cohesive soil by conducting a field experimental program, at various source vibration frequencies, in a flat secluded area.
- B-Assessing the efficiency of active and passive screening of open trenches.
- C-Selecting the isolation material to be added to the native soil.
- D-Experimentally investigating the efficiency of active and passive screening of trenches, filled with variable mixtures ratios.

* Corresponding author: Hasan A. Ajel, Department of Civil Engineering, College of Engineering, University of Basrah, Basrah, Iraq, e-mail: Ajelhasan730@gmail.com

Haider S. Al-Jubair: Department of Civil Engineering, College of Engineering, University of Basrah, Basrah, Iraq

Jaafar K. Ali: Department of Mechanical Engineering, College of Engineering, University of Basrah, Basrah, Iraq

Table 1: Experimental correlation between soil type and elastic parameters

| Soil type | Description | ν | E (MPa) |
|-----------|-------------|-----------|-----------|
| Clay | Soft | 0.35–0.40 | 1–15 |
| | Medium | 0.30–0.40 | 15–30 |
| | Stiff | 0.20–0.30 | 30–100 |
| Silt | | 0.30–0.35 | 2–20 |
| Sand | Loose | 0.15–0.25 | 10–20 |
| | Medium | 0.25–0.30 | 20–40 |
| | Dense | 0.25–0.35 | 40–80 |

2 Materials and methods

2.1 Soil profile

The geotechnical investigation program for the research site was conducted by the National Center Construction Laboratory-Basrah branch in 2002 [9]. The missing soil properties are predicted using correlative relations. The elastic parameters are obtained utilizing Table 1 [10], whereas the shear wave velocity (V_s) is calculated via the empirical formula [11]:

$$V_s = 58N^{0.39} \quad (2)$$

The main soil layers and their properties are listed in Table 2. The depth of groundwater at the site is (0.7 m) below the ground surface.

2.2 Equipment and devices used

The vertical sinusoidal harmonic excitation is induced via a mechanical oscillator (Vibratory Plate Compactor C-90). The (90 kg) mass plate compactor is powered by (5 hp) to produce a peak force of (15 kN) at a maximum operating velocity of (4,200 rpm). The unit is supplied by a speed regulator, which yields a steady range of operating frequency of (30–70 Hz).

To restrict the vibration waves at all, but, the vertical direction, the compactor is mounted on a (500 mm × 600 mm × 8 mm) steel plate and placed

**Figure 1:** The source of vibration.**Figure 2:** Measurement of the generated frequency.

concentrically above a (650 mm × 800 mm × 150 mm) concrete base, reinforced with ($\phi 12@150$ mm both directions), and constructed at an embedment depth

Table 2: Soil profile characteristics at the study site

| Layer | Depth (m) | Description | S.P.T | E (MPa) | ν | V_s (m/s) |
|-------|-----------|--|-------|-----------|-------|-------------|
| 1 | 0–3 | Medium stiff to stiff brown silty clay | 8 | 30 | 0.3 | 130.0 |
| 2 | 3–13 | Soft gray silty clay | 3 | 8 | 0.4 | 89 |
| 3 | 13–17 | Medium stiff to stiff gray silty clay | 8 | 30 | 0.3 | 130 |
| 4 | 17–19 | Very stiff gray (silty clay with sand) | 23 | 100 | 0.2 | 197 |
| 5 | 19–27 | Dense to very dense gray silty sand | 50 | 80 | 0.35 | 267.0 |

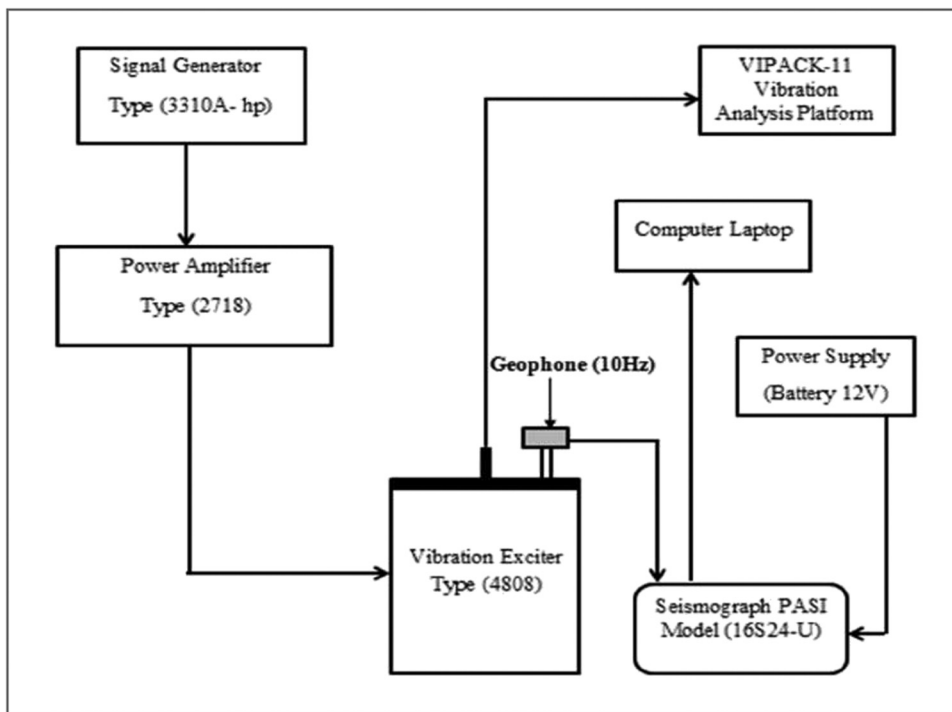


Figure 3: Schematic diagram of the geophone calibration.

of (0.25 m). The compactor is fixed to the steel plate and concrete base using four (10 mm) diameter threaded steel bolts (Figure 1). A digital tachometer is used to control the generated frequency (Figure 2).

Other devices used in the test program are receptors (geophones) connected to a data logger (24 channels seismograph), seismic cables (with takeout 5 m interval), laptop computer used to control the

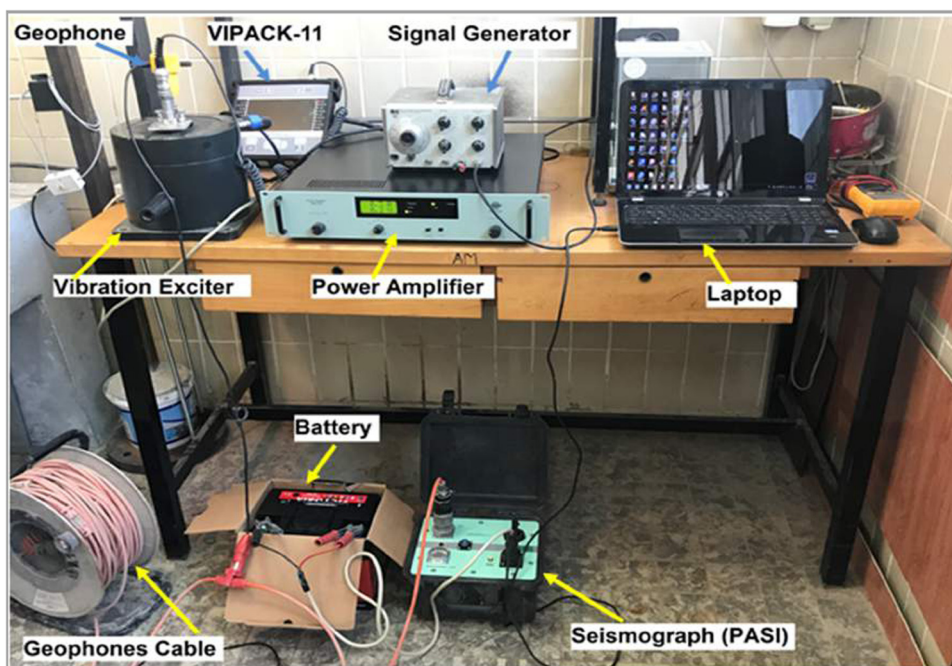


Figure 4: Calibration process in the laboratory.

Table 3: Geophone characteristics at sample frequencies

| Test no. | Frequency (Hz) | V (Volts) | Velocity (mm/s) | Sensitivity (V s/mm) |
|----------|----------------|-----------|-----------------|----------------------|
| 1 | 60 | 1.15 | 42.6 | 0.02699 |
| 2 | 30 | 0.58 | 21.5 | 0.02697 |
| Average | 45 | 0.865 | 32.05 | 0.02698 |

harmonic excitation through a seismic controller software, and (12 V) battery for power supply.

A sample of (4 s) of soil particle velocity measurements is obtained using vertical component geophones with a (2 ms) sampling interval resulting in (2,000) data points for each selected frequency.

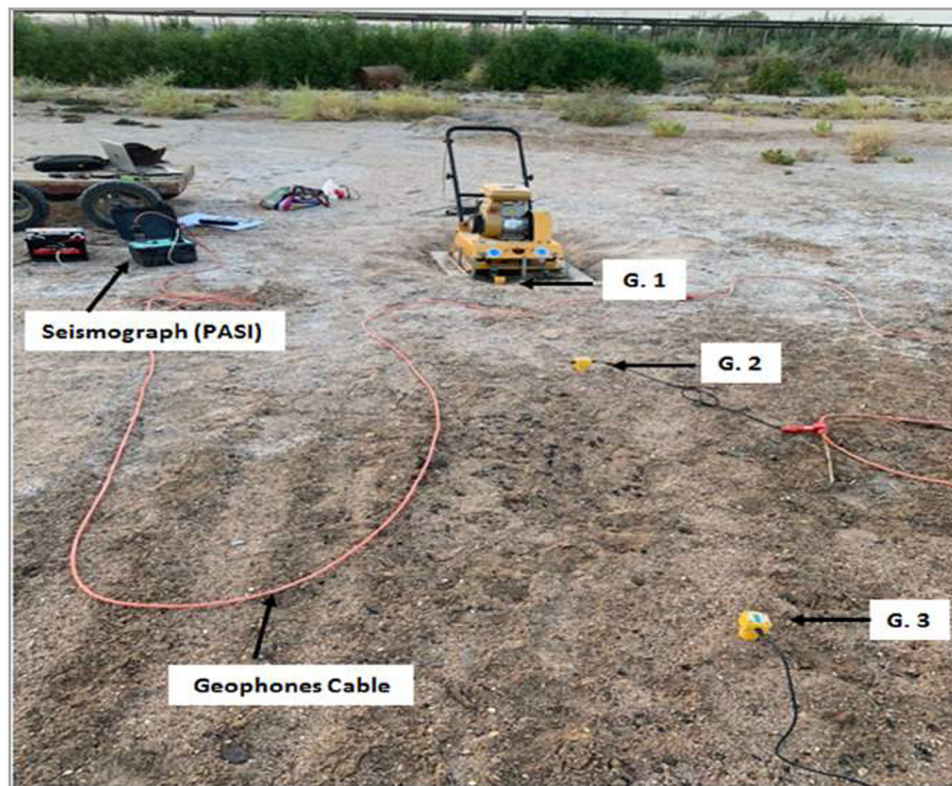
2.3 Calibration process

At the outset, the accuracy of the instruments' readings is investigated before starting the experimental study. The instruments subjected to the calibration process are the (24 Channel, 16S24-U, Ultra-Light) Exploration Seismograph system, manufactured by PASI Italy, and

Table 4: The measured peak particle velocities at different locations for various frequencies (no wave barrier)

| Distance (m) | Peak particle velocity (mm/s) | | | |
|--------------|-------------------------------|-------------|-------------|-------------|
| | $f = 30$ Hz | $f = 40$ Hz | $f = 55$ Hz | $f = 70$ Hz |
| 0.25 | 0.782796 | 3.739775 | 4.678678 | 6.092688 |
| 1.5 | 0.194568 | 1.280528 | 2.91173 | 2.683226 |
| 3 | 0.127827 | 1.212655 | 1.83482 | 2.357438 |
| 4.5 | 0.087103 | 0.975102 | 0.995463 | 1.790703 |
| 6 | 0.062216 | 1.180981 | 1.518082 | 2.035044 |
| 7.5 | 0.076922 | 0.565604 | 0.809945 | 0.949084 |
| 9 | 0.075791 | 0.499940 | 0.66515 | 0.782796 |
| 10.5 | 0.05656 | 0.283933 | 0.406104 | 0.490944 |
| 12 | 0.072397 | 0.205880 | 0.288458 | 0.357462 |
| 13.5 | 0.057692 | 0.186649 | 0.227373 | 0.298639 |
| 15 | 0.06561 | 0.178731 | 0.184387 | 0.230766 |
| 16.5 | 0.050904 | 0.144795 | 0.161763 | 0.192305 |

(10 Hz) Vertical Geophone. Figure 3 illustrates the calibration process, which is conducted in the Laboratory of Vibrations - Department of Mechanical Engineering using assistive devices (Figure 4) by entering a fixed-frequency signal and recording the vibration velocity reading each time to get the sensor's sensitivity, as listed in Table 3.

**Figure 5:** Arrangement of field test devices.

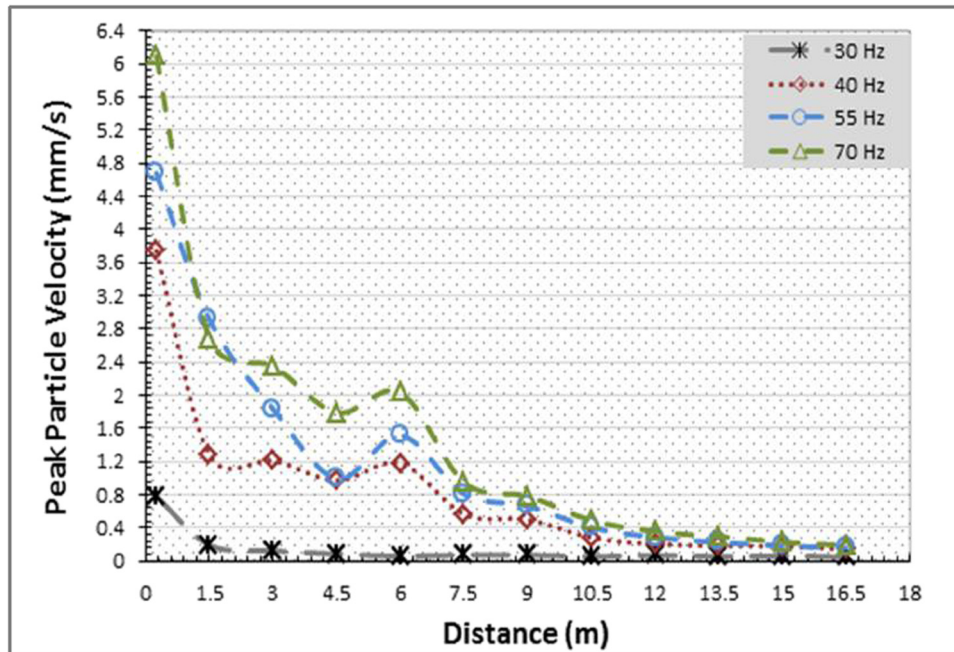


Figure 6: Attenuation of vibration velocity for various frequencies (no wave barrier).

3 Results

3.1 No wave barrier

This test stage consists of disturbing the ground with loads at different frequencies (30, 40, 55, and 70 Hz) and taking ground motion measurements at defined locations via (12) geophones placed on a line co-linear with

the vibrator, as shown in Figure 5. Geophone number (1) is positioned near the source of vibration, and the rest are placed at a spacing of 1.5 m.

It can be realized that the peak particle velocities are proportional with the excitation frequencies.

The results are listed in Table 4, whereas the attenuation of vibration velocity with horizontal distance is shown in Figure 6.



Figure 7: Open trench formation.

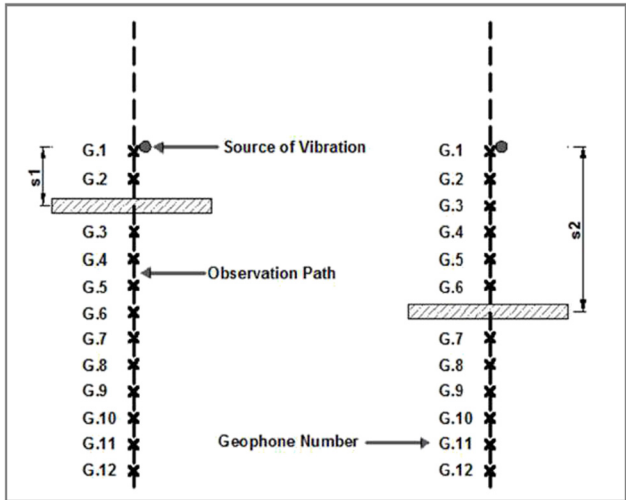


Figure 8: Field test configurations (trench barrier).

Table 5: The measured peak particle velocities at different locations for various frequencies (active open trench barrier)

| Distance (m) | Peak particle velocity, (mm/s) | | | |
|--------------|--------------------------------|---------------------|---------------------|---------------------|
| | $f = 30 \text{ Hz}$ | $f = 40 \text{ Hz}$ | $f = 55 \text{ Hz}$ | $f = 70 \text{ Hz}$ |
| 0.25 | 0.814107 | 4.038957 | 5.474053 | 7.494006 |
| 1.5 | 0.219861 | 1.549438 | 3.668779 | 3.488193 |
| 4.5 | 0.018988 | 0.034128 | 0.018913 | 0.019697 |
| 6 | 0.020282 | 0.042751 | 0.03947 | 0.03663 |
| 7.5 | 0.016922 | 0.020927 | 0.021868 | 0.018032 |
| 9 | 0.018038 | 0.022947 | 0.023945 | 0.016438 |
| 10.5 | 0.022624 | 0.032652 | 0.033706 | 0.022583 |
| 12 | 0.019185 | 0.020176 | 0.025355 | 0.016943 |
| 13.5 | 0.018403 | 0.019038 | 0.022003 | 0.023413 |
| 15 | 0.016927 | 0.017158 | 0.016963 | 0.013984 |
| 16.5 | 0.015831 | 0.024615 | 0.019088 | 0.022499 |

3.2 Open trench barrier

In this phase, a 0.4 m wide, 3 m long, and 2 m deep trench is mechanically dug, dynamic loading is applied at the same previous frequencies, and the ground motion measurements are recorded at the same predefined locations (Figure 7). Two positions of the vibrating source with respect to the trench are considered to examine the active and passive vibration screening. Figure 8 shows the field test configurations.

The results are listed in Table 5 for the active isolation, whereas the attenuation of vibration velocity is expressed in terms of amplitude reduction ratio (A_r), as shown in Figure 9.

The values listed in Table 5 reveal increased velocities at the points before the barrier due to the reflected

Table 6: The measured peak particle velocities at different locations for various frequencies (passive open trench barrier)

| Distance (m) | Peak particle velocity, (mm/s) | | | |
|--------------|--------------------------------|---------------------|---------------------|---------------------|
| | $f = 30 \text{ Hz}$ | $f = 40 \text{ Hz}$ | $f = 55 \text{ Hz}$ | $f = 70 \text{ Hz}$ |
| 0.25 | 0.808158 | 3.404317 | 5.155903 | 6.372951 |
| 1.5 | 0.191279 | 1.234557 | 3.313548 | 2.973014 |
| 3 | 0.124784 | 1.43457 | 2.209123 | 2.909078 |
| 4.5 | 0.08658 | 1.073587 | 1.088041 | 2.121983 |
| 6 | 0.059926 | 1.184523 | 1.52719 | 2.09813 |
| 7.5 | 0.070537 | 0.529405 | 0.771877 | 0.857971 |
| 10.5 | 0.01923 | 0.072118 | 0.098277 | 0.05744 |
| 12 | 0.032035 | 0.054681 | 0.038941 | 0.038963 |
| 13.5 | 0.027403 | 0.063833 | 0.061163 | 0.042705 |
| 15 | 0.03497 | 0.049151 | 0.046649 | 0.041766 |
| 16.5 | 0.026979 | 0.038081 | 0.038499 | 0.030384 |

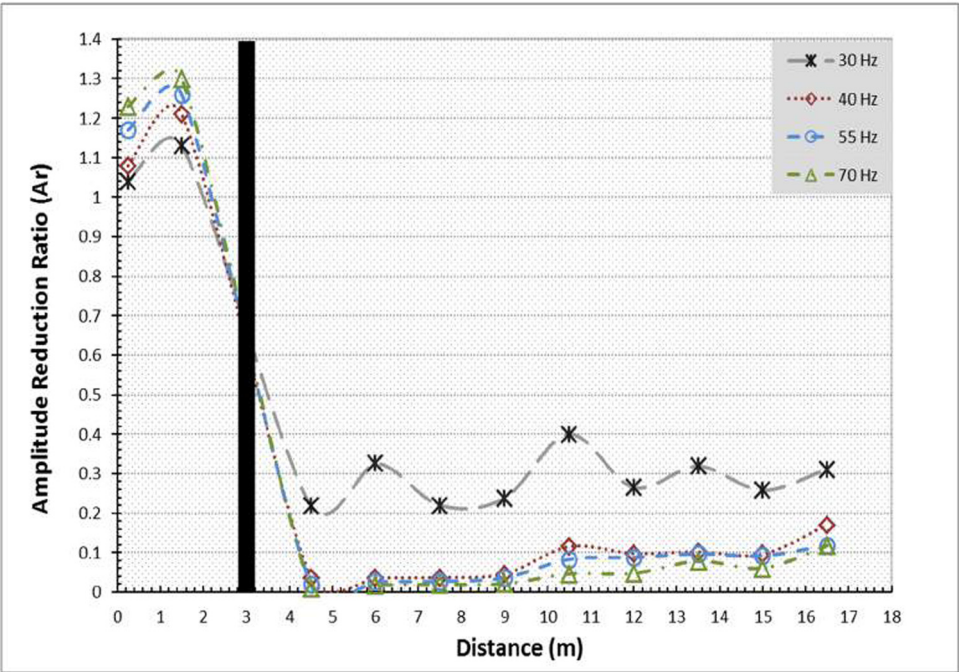


Figure 9: Attenuation of vibration velocity due to an open trench barrier (active screening).

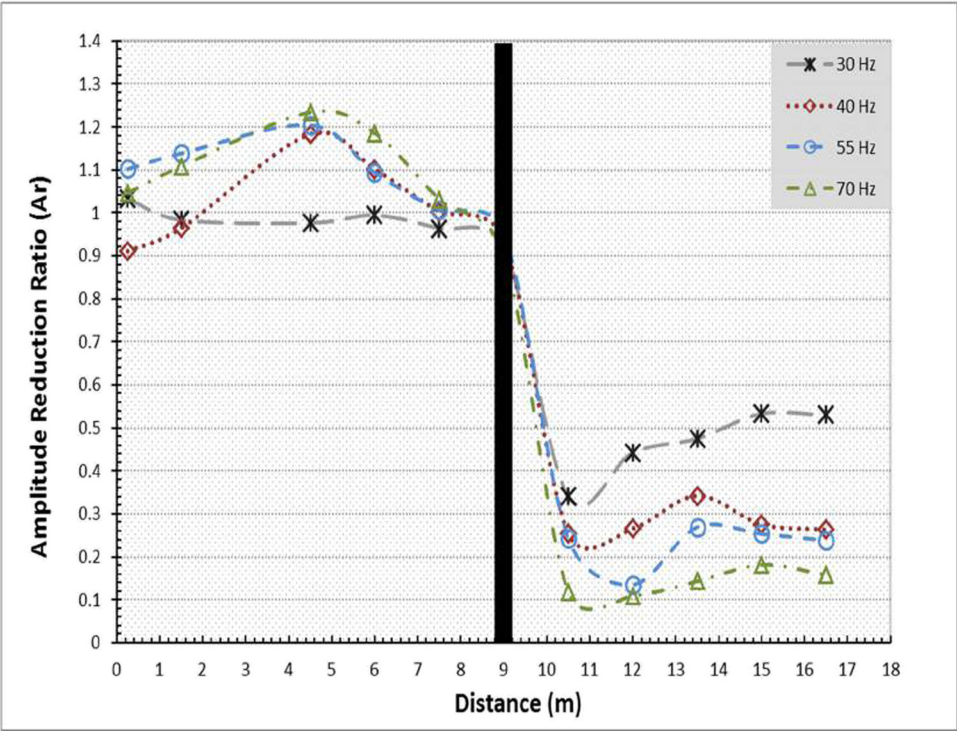


Figure 10: Attenuation of vibration velocity due to an open trench barrier (passive screening).



Figure 11: Production of rubber material in the factory.

Table 7: Properties of tire chips used in the study

| Average loose density (kg/m ³) | Average compacted density (kg/m ³) | Elastic modulus E (kPa) | Poisson's ratio (ν) |
|--|--|---------------------------|---------------------------|
| 320–490 | 570–730 | 580–770 | 0.32 |



Figure 12: Determination of the mixture densities.



Figure 13: Trench filling stages.

Table 8: The measured peak particle velocities at different locations for various frequencies (active in-filled with 20% rubber trench barrier)

| Distance (m) | Peak particle velocity (mm/s) | | | |
|--------------|-------------------------------|-------------|-------------|-------------|
| | $f = 30$ Hz | $f = 40$ Hz | $f = 55$ Hz | $f = 70$ Hz |
| 0.25 | 0.849333 | 3.937983 | 4.814359 | 6.86524 |
| 1.5 | 0.200988 | 1.343273 | 2.975788 | 2.868368 |
| 4.5 | 0.072077 | 0.754728 | 0.725692 | 1.215887 |
| 6 | 0.053941 | 0.949508 | 1.021669 | 1.349234 |
| 7.5 | 0.069236 | 0.403275 | 0.455594 | 0.558061 |
| 9 | 0.070652 | 0.4154 | 0.364502 | 0.462554 |
| 10.5 | 0.051056 | 0.2686 | 0.268434 | 0.283274 |
| 12 | 0.068197 | 0.190027 | 0.259323 | 0.243431 |
| 13.5 | 0.053595 | 0.159211 | 0.179397 | 0.179482 |
| 15 | 0.056818 | 0.147453 | 0.127595 | 0.146767 |
| 16.5 | 0.044999 | 0.120614 | 0.113719 | 0.104613 |

Table 9: The measured peak particle velocities at different locations for various frequencies (active in-filled with 30% rubber trench barrier)

| Distance (m) | Peak particle velocity (mm/s) | | | |
|--------------|-------------------------------|-------------|-------------|-------------|
| | $f = 30$ Hz | $f = 40$ Hz | $f = 55$ Hz | $f = 70$ Hz |
| 0.25 | 0.800017 | 5.048696 | 5.77816 | 8.462743 |
| 1.5 | 0.191065 | 1.422666 | 3.502811 | 2.930082 |
| 4.5 | 0.070117 | 0.652343 | 0.647847 | 1.015328 |
| 6 | 0.054936 | 0.935336 | 0.776195 | 0.982315 |
| 7.5 | 0.061537 | 0.34219 | 0.319118 | 0.370996 |
| 9 | 0.062375 | 0.375954 | 0.337231 | 0.321729 |
| 10.5 | 0.054976 | 0.26207 | 0.258688 | 0.261182 |
| 12 | 0.069501 | 0.180968 | 0.242016 | 0.220554 |
| 13.5 | 0.049557 | 0.153612 | 0.173485 | 0.167476 |
| 15 | 0.055112 | 0.13655 | 0.107497 | 0.128767 |
| 16.5 | 0.043879 | 0.110188 | 0.107895 | 0.082883 |

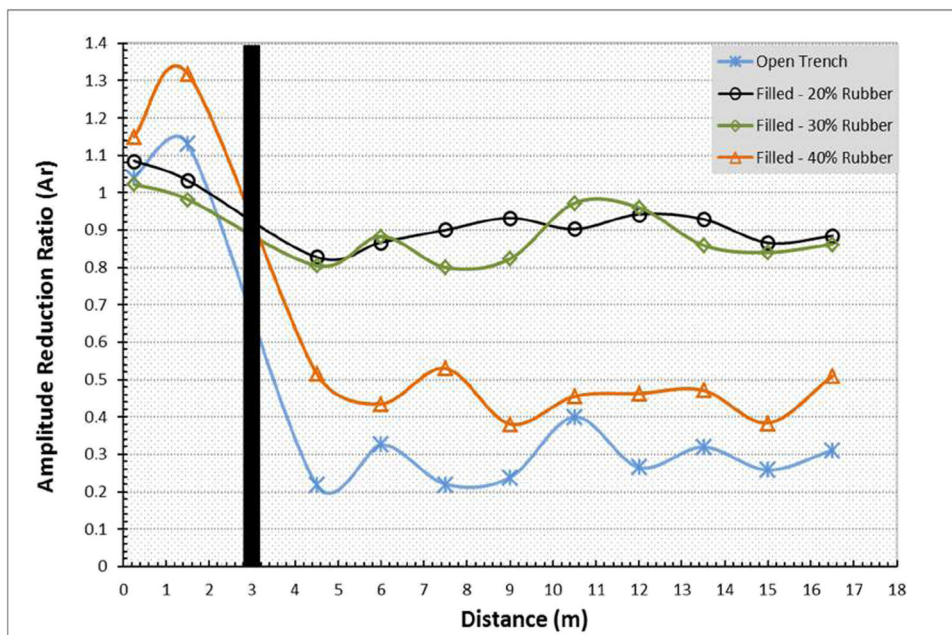
Table 10: The measured peak particle velocities at different locations for various frequencies (active in-filled with 40% rubber trench barrier)

| Distance (m) | Peak particle velocity (mm/s) | | | |
|--------------|-------------------------------|-------------|-------------|-------------|
| | $f = 30$ Hz | $f = 40$ Hz | $f = 55$ Hz | $f = 70$ Hz |
| 0.25 | 0.899432 | 4.543826 | 5.300942 | 7.097981 |
| 1.5 | 0.25644 | 1.271564 | 3.029464 | 3.241337 |
| 4.5 | 0.044945 | 0.498082 | 0.373298 | 0.653606 |
| 6 | 0.027063 | 0.527898 | 0.652775 | 0.771281 |
| 7.5 | 0.040768 | 0.23416 | 0.379054 | 0.370142 |
| 9 | 0.028876 | 0.198976 | 0.274706 | 0.320163 |
| 10.5 | 0.025734 | 0.128621 | 0.170726 | 0.203250 |
| 12 | 0.033519 | 0.089146 | 0.128075 | 0.148704 |
| 13.5 | 0.027172 | 0.084738 | 0.094814 | 0.107211 |
| 15 | 0.025194 | 0.06756 | 0.091087 | 0.104536 |
| 16.5 | 0.02591 | 0.064723 | 0.080719 | 0.083460 |

waves. This increase is proportional to the vibration frequency. A great reduction in velocity can be noted in Figure 9 due to the presence of the open trench. The reduction is proportional with the frequency, which means that the efficiency of screening is more pronounced at high vibration frequencies. Increasing and fluctuating trends of (A_r) are reported away from the barrier.

The results are listed in Table 6 for the passive isolation, whereas the attenuation of vibration velocity is expressed in terms of amplitude reduction ratio (A_r), as shown in Figure 10.

It can be deduced from Table 6 that, the reflected wave effects cover longer distances compared to the active case. The curves presented in Figure 10 show

**Figure 14:** Attenuation of vibration due to active trench barriers ($f = 30$ Hz).

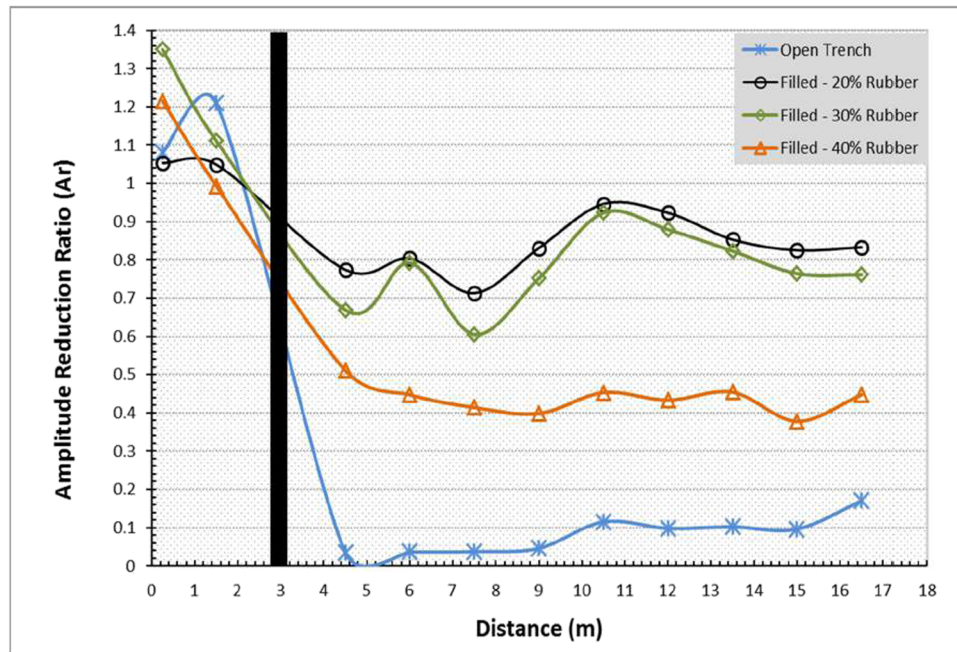


Figure 15: Attenuation of vibration due to active trench barriers ($f = 40$ Hz).

behavior similar to that of the previous case. The passive screening is less effective than the active one for all frequencies except at 30 Hz. The difference in behavior could be attributed to the considerable interaction effect of the waves reflected from the active barrier on the source induced waves, compared to its counterpart for the passive one.

3.3 In-filled trench barrier

The open trench is filled with a compacted mixture of the excavated soil and rubber material at different percentages, the harmonic excitation is applied, and measurements of ground motion are recorded at the same frequencies and the specified locations.

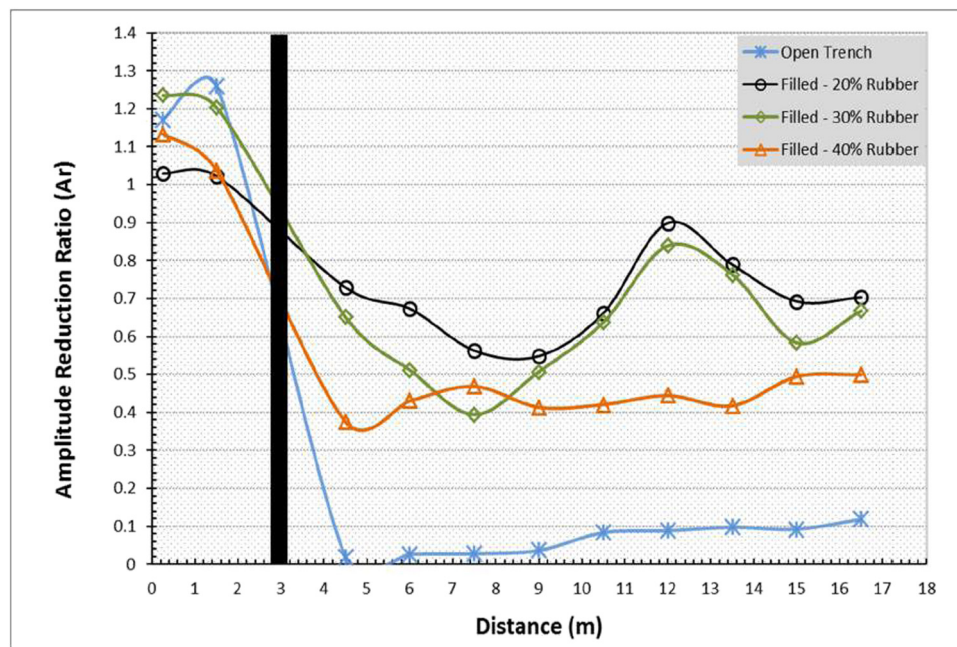


Figure 16: Attenuation of vibration due to active trench barriers ($f = 55$ Hz).

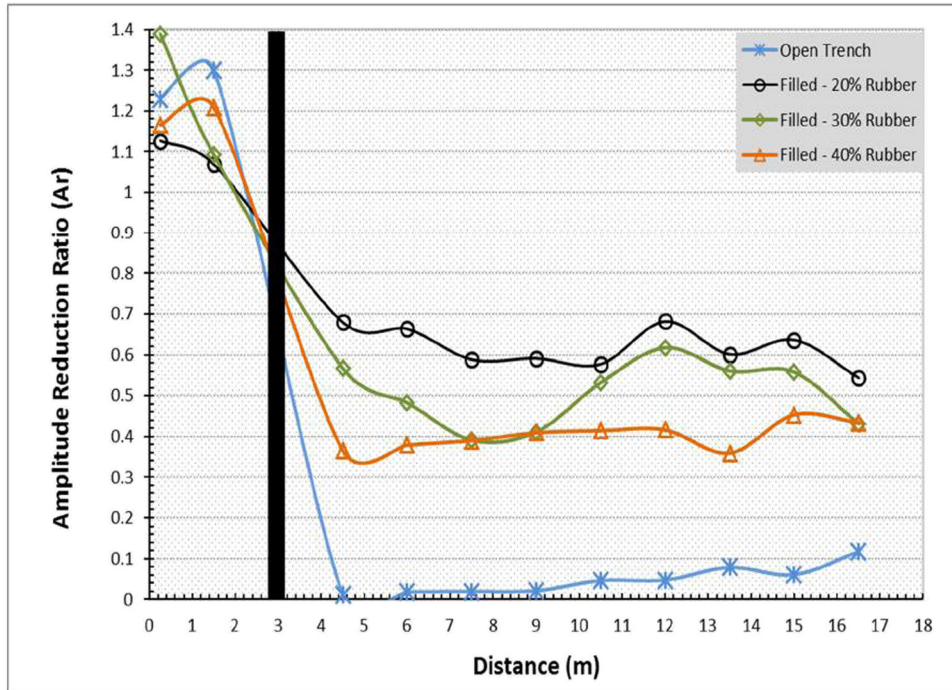


Figure 17: Attenuation of vibration due to active trench barriers ($f = 70$ Hz).

Table 11: The measured peak particle velocities at different locations for various frequencies (passive in-filled with 20% rubber trench barrier)

| Distance (m) | Peak particle velocity (mm/s) | | | |
|--------------|-------------------------------|-------------|-------------|-------------|
| | $f = 30$ Hz | $f = 40$ Hz | $f = 55$ Hz | $f = 70$ Hz |
| 0.25 | 0.804714 | 3.82205 | 4.790966 | 6.598381 |
| 1.5 | 0.213635 | 1.326627 | 2.931529 | 3.064244 |
| 3 | 0.147895 | 1.214231 | 1.867846 | 2.600254 |
| 4.5 | 0.093635 | 1.000454 | 1.008404 | 1.801447 |
| 6 | 0.069681 | 1.262468 | 1.621311 | 2.067604 |
| 7.5 | 0.079999 | 0.570128 | 0.859351 | 1.018367 |
| 10.5 | 0.052595 | 0.256675 | 0.329472 | 0.365753 |
| 12 | 0.068407 | 0.182203 | 0.252689 | 0.284754 |
| 13.5 | 0.052442 | 0.166675 | 0.203044 | 0.244406 |
| 15 | 0.061148 | 0.161572 | 0.161062 | 0.189551 |
| 16.5 | 0.048404 | 0.130358 | 0.141801 | 0.158401 |

Table 12: The measured peak particle velocities at different locations for various frequencies (passive in-filled with 30% rubber trench barrier)

| Distance (m) | Peak particle velocity (mm/s) | | | |
|--------------|-------------------------------|-------------|-------------|-------------|
| | $f = 30$ Hz | $f = 40$ Hz | $f = 55$ Hz | $f = 70$ Hz |
| 0.25 | 0.844636 | 5.13845 | 6.9338 | 6.970035 |
| 1.5 | 0.187758 | 1.271564 | 3.08061 | 3.437212 |
| 3 | 0.125554 | 1.202468 | 2.007293 | 3.123605 |
| 4.5 | 0.096144 | 1.063348 | 1.060168 | 1.761156 |
| 6 | 0.064474 | 1.273097 | 1.510491 | 2.006736 |
| 7.5 | 0.089306 | 0.668543 | 0.886079 | 1.005554 |
| 10.5 | 0.051526 | 0.250712 | 0.31274 | 0.315971 |
| 12 | 0.06465 | 0.17788 | 0.237141 | 0.26016 |
| 13.5 | 0.050884 | 0.151372 | 0.191016 | 0.231893 |
| 15 | 0.059114 | 0.155853 | 0.149906 | 0.182997 |
| 16.5 | 0.046526 | 0.120759 | 0.139277 | 0.154613 |

The rubber material used in this study is purchased from the Unit of Recycling Scrap Tires in Al-Diwaniyah Tires Factory. The tire chips are obtained by rotating, chopping them, and turning them into various rubber products as shown in Figure 11. They are basically flat, irregular tire pieces, and more finely and uniformly sized. Secondary shredding results in the production of chips are more equidimensional.

Tire chips resulted from secondary shredding are normally sized from 13 to 25 mm. They are nonreactive under normal environmental conditions and have an absorption range of (2–3.8%). Additional properties are listed in Table 7. Three different rubber contents (20, 30, and 40%) by weight are mixed with the excavated natural soil. The densities of the mixture are determined in the soil mechanics laboratory, as shown in Figure 12, as

Table 13: The measured peak particle velocities at different locations for various frequencies (passive in-filled with 40% rubber trench barrier)

| Distance (m) | Peak particle velocity (mm/s) | | | |
|--------------|-------------------------------|---------------------|---------------------|---------------------|
| | $f = 30 \text{ Hz}$ | $f = 40 \text{ Hz}$ | $f = 55 \text{ Hz}$ | $f = 70 \text{ Hz}$ |
| 0.25 | 0.79078 | 3.915544 | 5.118473 | 6.220634 |
| 1.5 | 0.22064 | 1.362481 | 2.920465 | 2.806654 |
| 3 | 0.14585 | 1.416381 | 1.849498 | 2.371582 |
| 4.5 | 0.102171 | 1.089188 | 1.009399 | 1.792493 |
| 6 | 0.072419 | 1.303803 | 1.759457 | 2.08999 |
| 7.5 | 0.078152 | 0.645014 | 0.984893 | 1.037823 |
| 10.5 | 0.046039 | 0.201876 | 0.264779 | 0.236438 |
| 12 | 0.060741 | 0.15338 | 0.288458 | 0.181948 |
| 13.5 | 0.046211 | 0.138866 | 0.134286 | 0.157084 |
| 15 | 0.053668 | 0.13773 | 0.113951 | 0.123921 |
| 16.5 | 0.044591 | 0.120035 | 0.107895 | 0.118652 |

1,143, 1,135, and 1,014 kg/m³. The filling stages of the trench are shown in Figure 13.

The measured velocities are listed in Tables 8–10 for the active case and the wave attenuation is shown in Figures 14–17.

The peak particle velocities before the in-filled barrier are affected by the reflected waves, as can be concluded from Tables 8–10. Figures 14–17 illustrate reductions in velocities due to the barrier, which are proportional with the vibration frequency. In general, the efficiency of screening is increased with the rubber

content of the filling material. Similar to the open trench barrier, increasing and fluctuating relations of (A_r) are resulted away from the barrier.

For the passive case, the measured velocities are listed in Tables 11–13, whereas the wave attenuation is shown in 18–21. Tables 11–13 list increased velocity values over larger range than the active isolation, before the barrier. In Comparison with the active case, similar findings are obtained from Figures 18–21 regarding the reduced velocities, the efficiency of screening, and the trend of curves.

3.4 Targeted point

A targeted point at a distance of (10.5 m) from the vibration source is selected for protection. The peak particle velocities and amplitude reduction ratios for various frequencies and screening methods are listed in Table 14.

3.5 Isolation cost

The feasibility of the filling mix from the economical stand point is studied. An excavation unit price of 4.5 USD/m³, backfilling unit price of 7 USD/m³, and rubber unit price of 75 USD/ton are adopted. For 40%

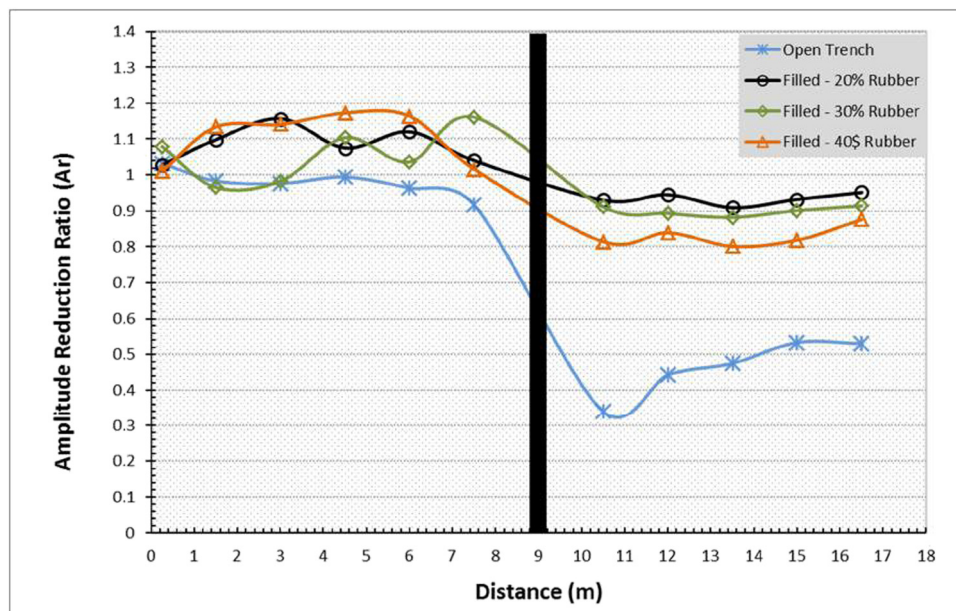


Figure 18: Attenuation of vibration due to passive trench barriers ($f = 30 \text{ Hz}$).

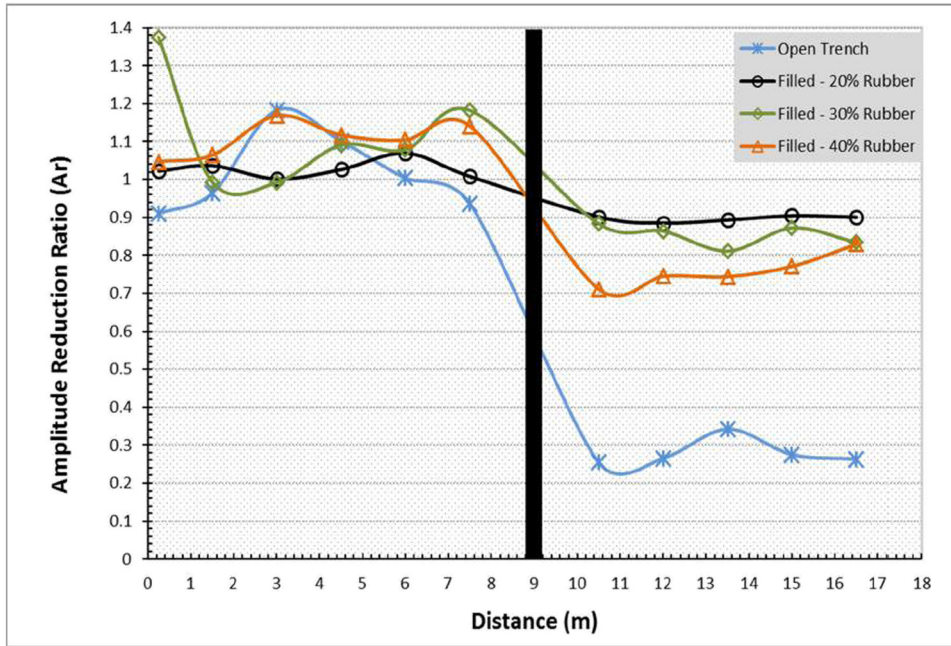


Figure 19: Attenuation of vibration due to passive trench barriers ($f = 40$ Hz).

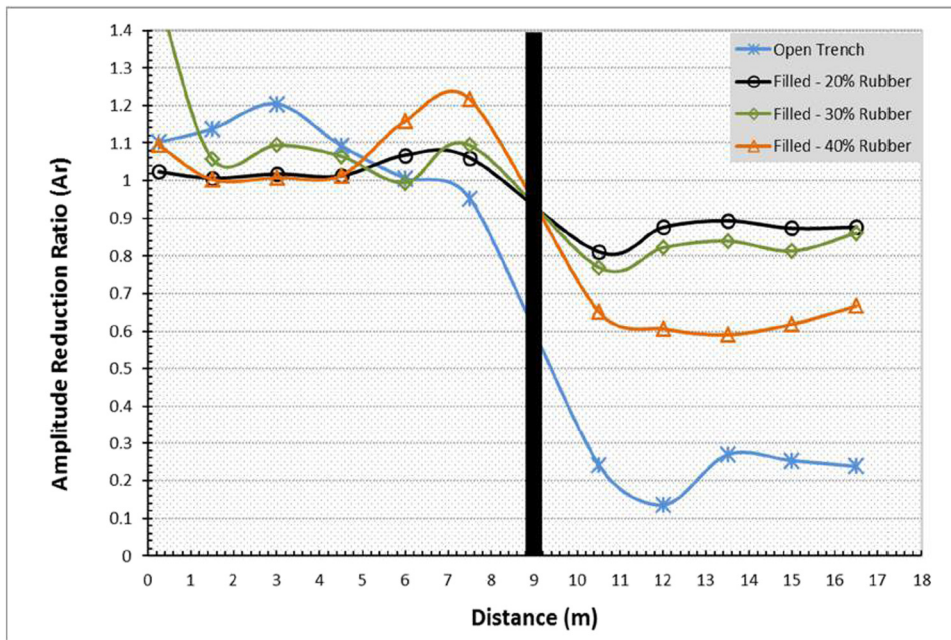


Figure 20: Attenuation of vibration due to passive trench barriers ($f = 55$ Hz).

rubber content, the screening process costs ≈ 42 USD/m³, which is a very competitive price.

4 Conclusion

The following conclusions can be drawn:

1. Excavation of an active open trench barrier reduces the vertical components of peak particle velocities by 60–95.4%. High attenuation rates are associated with high source vibration frequencies.
2. Except few particular values at low frequencies, the active screening proved to be more powerful than the passive one. Those frequencies usually do not

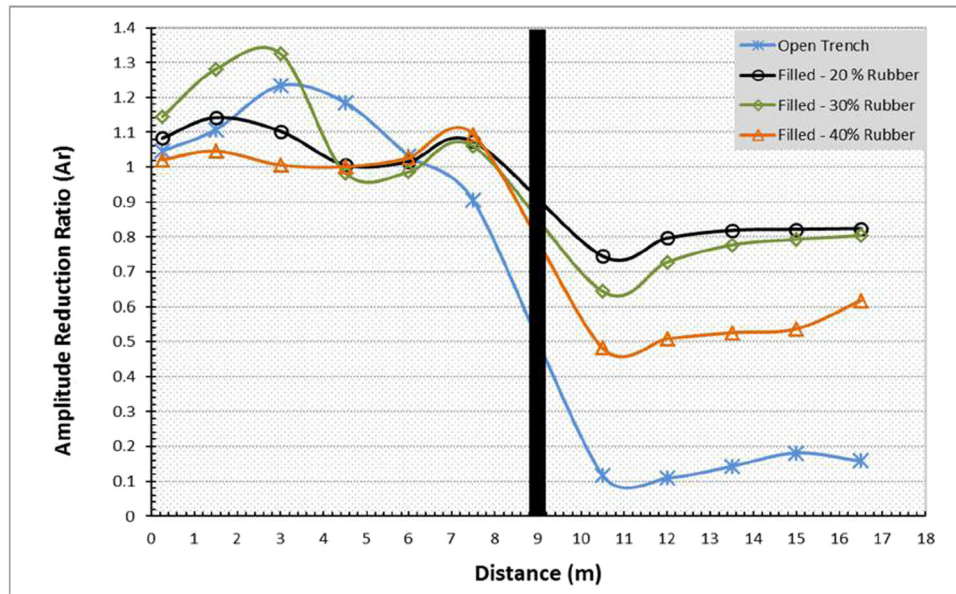


Figure 21: Attenuation of vibration due to passive trench barriers ($f = 70$ Hz).

Table 14: Peak particle velocities and amplitude reduction ratios at the targeted point

| Case | Distance (m) | P.P.V. (mm/s) and A_r | | | |
|------------------------------|--------------|-------------------------|-------------|-------------|-------------|
| | | $f = 30$ Hz | $f = 40$ Hz | $f = 55$ Hz | $f = 70$ Hz |
| No barrier | 0.25 | 0.782796 | 3.739775 | 4.678678 | 6.092688 |
| | 10.5 | 0.056560 | 0.283933 | 0.406104 | 0.490944 |
| Open trench-active, A_r | 10.5 | 0.022624 | 0.032652 | 0.033706 | 0.022583 |
| | | 0.400 | 0.115 | 0.083 | 0.046 |
| Open trench-passive, A_r | 10.5 | 0.019230 | 0.072118 | 0.098277 | 0.057440 |
| | | 0.340 | 0.254 | 0.242 | 0.117 |
| In-filled 20%-active, A_r | 10.5 | 0.051056 | 0.268600 | 0.268434 | 0.283274 |
| | | 0.903 | 0.946 | 0.661 | 0.577 |
| In-filled 20%-passive, A_r | 10.5 | 0.052595 | 0.256675 | 0.329472 | 0.365753 |
| | | 0.930 | 0.904 | 0.811 | 0.745 |
| In-filled 30%-active, A_r | 10.5 | 0.054976 | 0.262070 | 0.258688 | 0.261182 |
| | | 0.972 | 0.923 | 0.637 | 0.532 |
| In-filled 30%-passive, A_r | 10.5 | 0.051526 | 0.250712 | 0.312740 | 0.315971 |
| | | 0.911 | 0.883 | 0.770 | 0.644 |
| In-filled 40%-active, A_r | 10.5 | 0.025734 | 0.128621 | 0.170726 | 0.203250 |
| | | 0.455 | 0.453 | 0.420 | 0.414 |
| In-filled 40%-passive, A_r | 10.5 | 0.046039 | 0.201876 | 0.264779 | 0.236438 |
| | A_r | 0.814 | 0.711 | 0.652 | 0.482 |

demonstrate the screening effect, considerably. Construction of a passive open trench barrier decreases the velocities by 66–88.3%.

- Using active barriers, filled with (native cohesive soil + rubber) mixtures with a rubber content ranging from 20 to 40%, achieved screening rates of 2.8–58.6%.

Better screening is associated with high rubber content and high frequency.

- Utilizing passive in-filled trenches produced mitigation rates of 7–51.8%.
- The locally available tire chips proved to be economical and effective in vibration isolation when it is

mixed with the original cohesive soil to form a trench filling material.

Conflict of interest: No potential conflict of interest was reported by the authors.

References

- [1] Woods RD. Screening of surface wave in soils. *J Soil Mechanics Found Division*. 1968;94(4):951–79.
- [2] Beskos DE, Dasgupta B, Vardoulakis IG. Vibration isolation using open or filled trenches. *Comput Mech*. 1986;1(1):43–63. doi: 10.1007/bf00298637.
- [3] Celebi E, Firat S, Beyhan G, Cankaya I, Vural S, Kirtel O. Field experiments on wave propagation and vibration isolation by using wave barriers. *Soil Dynam Earthquake Eng*. 2009;29(5):824–33. doi: 10.1016/j.soildyn.2008.08.007.
- [4] Murillo C, Thorel L, Caicedo B. Ground vibration isolation with geofoam barriers: Centrifuge modeling. *Geotextiles Geomembranes*. 2009;27(6):423–34. doi: 10.1016/j.geotextmem.2009.03.006.
- [5] Alzawi A, Hesham El Naggar M. Full scale experimental study on vibration scattering using open and in-filled (GeoFoam) wave barriers. *Soil Dynam Earthquake Eng*. 2011;31(3):306–17. doi: 10.1016/j.soildyn.2010.08.010.
- [6] Garinei A, Risitano G, Scappaticci L. Experimental evaluation of the efficiency of trenches for the mitigation of train-induced vibrations. *Transport Res D Transport Environ*. 2014;32:303–15. doi: 10.1016/j.trd.2014.08.016.
- [7] Ulgen D, Toygar O. Screening effectiveness of open and in-filled wave barriers: A full-scale experimental study. *Construct Building Materials*. 2015;86:12–20. doi: 10.1016/j.conbuildmat.2015.03.098.
- [8] Mahdavisefat E, Salehzadeh H, Heshmati AA. Full-scale experimental study on screening effectiveness of SRM-filled trench barriers. *J Géotechnique*. 2018;68(10):869–82. doi: 10.1680/jgeot.17.p.007.
- [9] National Center Construction Laboratory-Basrah Construction Laboratory. Subsoil Investigation for the Site of Garbat Ali/ Basrah University. Report No.2/1/11.; 2002.
- [10] Bowles JE. Foundation analysis and design. 5th ed. New York: The McGraw-Hill Companies; 1997.
- [11] Dikmen N. Statistical correlations of shear wave velocity and penetration resistance for soils. *J Geophys Eng*. 2009;6(1):61–72. doi: 10.1088/1742-2132/6/1/007.